JOURNAL OF SOLID STATE CHEMISTRY **134,** 148–157 (1997)
ARTICLE NO. SC977566

Syntheses and Crystal Structures of Two New Hydrated Rubidium Zinc Phosphates: $RbZn_2(HPO_4)_2(H_2PO_4)\cdot 2H_2O$, a Layered Phase Containing Octahedral and Tetrahedral Zinc Centers, and $RbZn(HPO_4)(H_2PO_4)\cdot H_2O$ Containing One-Dimensional Chains of 4-Rings

William T. A. Harrison,[1] Zsolt Bircsak, and Lakshitha Hannooman

Department of Chemistry, University of Western Australia, Nedlands, WA 6907, Australia

Received November 26, 1996; in revised form July 21, 1997; accepted July 24, 1997

The solution-mediated syntheses, single crystal structures, and physical properties (TGA, IR) of $RbZn_2(HPO_4)_2(H_2PO_4)\cdot 2H_2O$ and $RbZn(HPO_4)(H_2PO_4)\cdot H_2O$ are reported. $RbZn_2(HPO_4)_2(H_2PO_4)\cdot 2H_2O$ is a new noncentrosymmetric layered phase built up from ZnO_6, ZnO_4, and PO_4 polyhedra-sharing vertices as Zn–O–P and Zn–O–Zn bonds. Eleven-coordinate rubidium cations provide interlayer charge compensation for the anionic Zn/P/O/H sheets. $RbZn(HPO_4)(H_2PO_4)\cdot H_2O$ is isostructural with $NH_4Zn(HPO_4)(H_2PO_4)\cdot H_2O$ and consists of infinite chains of tetrahedral 4-rings connected by Zn–O–P bonds. Crystal data for $RbZn_2(HPO_4)_2(H_2PO_4)\cdot 2H_2O$ is: $M_r = 541.20$, orthorhombic, space group $P2_12_12_1$ (No. 19), $a = 7.6458(9)$, $b = 9.965(2)$, $c = 15.603(3)$ Å, $V = 1188.8(3)$ Å^3, $Z = 4$, $R(F) = 3.90\%$, $R_w(F) = 3.91\%$, (1695 observed reflections with $I > 3\sigma(I)$). Crystal data for $RbZn(HPO_4)(H_2PO_4)\cdot H_2O$ is $M_r = 361.83$, triclinic, space group $P\bar{1}$ (No. 2), $a = 7.712(2)$, $b = 7.9824(7)$, $c = 8.0422(9)$ Å, $\alpha = 64.313(7)^\circ$, $\beta = 84.90(2)^\circ$, $\gamma = 72.364(9)^\circ$, $V = 424.6(2)$ Å^3, $Z = 2$, $R(F) = 3.97\%$, $R_w(F) = 4.24\%$, (1794 observed reflections with $I > 3\sigma(I)$). © 1997 Academic Press

INTRODUCTION

The sodium/zinc/phosphate (NaZnPO) system has yielded a striking variety of new crystalline phases under ambient and mild hydrothermal conditions (1). Most of these phases consist of networks of vertex-linked ZnO_4 and PO_4 tetrahedra, akin to the bonding situation of the AlO_4 and SiO_4 units in aluminosilicate zeolites. The resulting NaZnPO materials include direct analogues of aluminosilicate zeolites (2, 3), continuous frameworks with no zeolitic counterparts (4, 5), and layered and chain-like structures with respect to Zn/P/O connectivity (6, 7). Using small organic molecules as templating agents leads to a wide variety of novel open-framework structures (8–12).

We are now exploring the rubidium/zinc/phosphate (RbZnPO) phase space by way of mild-condition solution-phase reactions. One interesting phase already prepared as a powder is $Rb_3Zn_4O(PO_4)_3\cdot 3.5H_2O$, consisting of a three-dimensional zincophosphate framework surrounding a network of spheroidal cavities interconnected by 8-ring windows (4). Unlike most zincophosphate frameworks which collapse upon dehydration, this material shows significant thermal stability, to at least 350°C. Previous reports have described the use of high-temperature synthetic methods to prepare $Rb_2Zn_3(P_2O_7)_2$ (13) and $RbZnPO_4$ (14).

In this paper we report the syntheses and single-crystal structures of two new rubidium zinc phosphate hydrates, $RbZn_2(HPO_4)_2(H_2PO_4)\cdot 2H_2O$ and $RbZn(HPO_4)\cdot(H_2PO_4)\cdot H_2O$.

EXPERIMENTAL

Synthesis

$RbZn_2(HPO_4)_2(H_2PO_4)\cdot 2H_2O$ was prepared at ambient conditions from the reaction of 85% phosphoric acid (4.8 g), 25% tetramethylammonium hydroxide (TMAOH) solution (11.66 g), and 50% rubidium hydroxide solution (2.46 g). This mixture was shaken together in a plastic bottle until homogeneous, followed by the addition of zinc nitrate (5.32 g), resulting in a white gel. The bottle was shaken again to homogenize the gel which formed a white precipitate. After the initial white powder was filtered off, well-faceted transparent plates of the title compound formed over the course of a few minutes, and these were filtered off in turn. This material appears to be indefinitely stable in ambient conditions. We have not been able to prepare good-quality

[1] To whom correspondence should be addressed. E-mail: wtah@chem.uwa.edu.au.

0022-4596/97 $25.00

single crystals of $RbZn_2(HPO_4)_2(H_2PO_4)\cdot 2H_2O$ in the absence of TMAOH.

$RbZn(HPO_4)(H_2PO_4)\cdot H_2O$ was prepared from 10 g ZnO, 7.13 ml 85% H_3PO_4 solution, and 7.24 ml 50% RbOH solution, which were mixed together in a plastic bottle until homogeneous. TMAOH (11 ml) was added to the mixture, and the bottle was shaken again until a homogeneous white gel had formed. This gel was heated to 100°C on a hotplate; while heating, 1 ml TMAOH and 2 ml H_3PO_4 were added to the mixture, resulting in a clear solution. Upon cooling, a powdery white precipitate formed, which was filtered off to result in a clear filtrate. The filtrate was allowed to evaporate at room temperature for 1 day, after which transparent, well-faceted, irregular crystals of $RbZn(HPO_4)\cdot(H_2PO_4)\cdot H_2O$ were recovered. After standing for several weeks, some poor-quality crystals of $RbZn_2(HPO_4)_2\cdot(H_2PO_4)\cdot 2H_2O$ crystallized from the same solution.

Physical Data

Powder X-ray data for well-ground, white powder samples of the title compounds were collected on a Siemens D5000 automated powder diffractometer (Cu$K\alpha$ radiation, $\lambda = 1.54178$ Å, $T = 25(2)$°C). A software "stripping" and peak-fitting routine established peak positions relative to the Cu$K\alpha_1$ wavelength ($\lambda = 1.54056$ Å), and *hkl* indices were assigned on the basis of comparison with LAZY-PULVERIX (15) simulations of the single-crystal structures. On the basis of this simulation, the pattern for $RbZn(HPO_4)(H_2PO_4)\cdot H_2O$ showed strong preferred orientation effects along [001]. The least-squares refinements were performed using the program UNITCELL (16). For $RbZn_2(HPO_4)_2(H_2PO_4)\cdot 2H_2O$: orthorhombic, $a = 7.653(5)$, $b = 9.959(6)$, $c = 15.586(6)$ Å, $V = 1188.0(8)$ Å^3. For $RbZn(HPO_4)(H_2PO_4)\cdot H_2O$: triclinic, $a = 7.703(2)$, $b = 7.988(2)$, $c = 8.046(2)$ Å, $\alpha = 64.32(2)^\circ$, $\beta = 84.99(2)^\circ$, $\gamma = 72.40(3)^\circ$, $V = 424.7(2)$ Å^3. Powder data for $RbZn_2(HPO_4)_2\cdot(H_2PO_4)\cdot 2H_2O$ are listed in Table 1 with similar data for $RbZn(HPO_4)(H_2PO_4)\cdot H_2O$ in Table 2. TGA data were collected under flowing O_2 gas on a Rigaku Thermoflex unit (heating rate: 20°C/min).

Crystal Structure Determinations

The structures of $RbZn_2(HPO_4)_2(H_2PO_4)\cdot 2H_2O$ and $RbZn(HPO_4)(H_2PO_4)\cdot H_2O$ were established from single-crystal X-ray diffraction data, as summarized in Table 3. In each case, a suitable crystal (for $RbZn_2(HPO_4)_2(H_2PO_4)\cdot 2H_2O$: transparent, faceted plate, dimensions $\sim 0.1\times 0.3\times 0.4$ mm; for $RbZn(HPO_4)(H_2PO_4)\cdot H_2O$: transparent, faceted rod, dimensions $\sim 0.20\times 0.05\times 0.05$ mm) was mounted on a thin glass fiber with cyanoacrylate adhesive, and room-temperature (25(2)°C) intensity data were collected on a Siemens P4 automated four-circle diffractometer (graphite-monochromated Mo$K\alpha$ radiation, $\lambda = 0.71073$ Å). Peak search, centering, indexing, and least-squares refinement routines led to an orthorhombic unit cell for $RbZn_2(HPO_4)_2(H_2PO_4)\cdot 2H_2O$ and a triclinic cell for $RbZn(HPO_4)(H_2PO_4)\cdot H_2O$. Data were collected using the $\omega/2\theta$ scan mode: Three standard reflections, rescanned every 100 observations, showed no significant variation in intensity over the course of each data collection. Crystal absorption (range of equivalent transmission factors 0.09–0.18 for $RbZn_2(HPO_4)_2(H_2PO_4)\cdot 2H_2O$; 0.41–0.85 for $RbZn(HPO_4)(H_2PO_4)\cdot H_2O$) was accounted for by the ψ scan method during data reduction, and redundant reflections were merged, resulting in 1695 observed reflections for $RbZn_2(HPO_4)_2(H_2PO_4)\cdot 2H_2O$ and 1794 observed reflections for $RbZn(HPO_4)(H_2PO_4)\cdot H_2O$ (observability criterion: $I > 3\sigma(I)$). The systematic absence conditions in the reduced data for $RbZn_2(HPO_4)_2(H_2PO_4)\cdot 2H_2O$ ($h00$, $h \neq 2n$; $0k0$, $k \neq 2n$; $00l$, $l \neq 2n$) indicated the noncentrosymmetric space group $P2_12_12_1$ (No. 19), thus, would-be Friedel equivalences were not merged for this data set.

TABLE 1
Powder X-Ray Data for $RbZn_2(HPO_4)_2(H_2PO_4)\cdot 2H_2O$

h	*k*	*l*	d_{obs} (Å)	d_{calc} (Å)	Δd	I_{rel}
0	0	2	7.783	7.793	− 0.010	41
1	1	1	5.658	5.655	− 0.003	56
1	0	2	5.462	5.460	0.001	6
1	1	2	4.791	4.788	0.003	37
1	0	3	4.293	4.298	− 0.005	6
0	2	2	4.199	4.196	0.003	16
1	2	1	4.031	4.032	− 0.001	13
1	1	3	3.947	3.946	0.001	73
0	0	4	3.903	3.896	0.007	50
1	2	2	3.680	3.679	0.001	100
0	2	3	3.595	3.595	0.000	22
2	1	0	3.564	3.572	− 0.008	12
1	0	4	3.473	3.472	0.001	62
2	0	2	3.437	3.435	0.002	12
1	1	4	3.285	3.279	0.006	25
1	2	3	3.252	3.254	− 0.002	69
2	0	3	3.080	3.081	− 0.001	72
1	3	0	3.043	3.046	− 0.002	27
1	3	1	2.984	2.989	− 0.005	64
2	1	3	2.944	2.943	0.001	67
1	0	5	2.893	2.887	0.006	14
0	3	3	2.799	2.797	0.001	54
1	1	5	2.774	2.773	0.001	32
1	3	3	2.628	2.627	0.000	27
0	1	6	2.516	2.514	0.002	90
2	2	4	2.394	2.394	0.000	36
1	3	5	2.180	2.178	0.001	30
2	2	6	1.9759	1.9732	0.0027	22
1	5	1	1.9110	1.9130	− 0.0020	18
3	3	3	1.8857	1.8849	0.0008	19
1	2	8	1.7673	1.7654	0.0019	18

TABLE 2
Powder X-Ray Data for $RbZn(HPO_4)(H_2PO_4)\cdot H_2O$

h	k	l	d_{obs} (Å)	d_{calc} (Å)	Δd	I_{rel}
0	0	1	7.242	7.242	−0.000	54
0	1	0	6.881	6.879	0.003	2
0	1	1	6.597	6.595	0.003	<1
1	1	0	5.973	5.971	0.002	13
1	1	1	5.604	5.606	−0.002	7
1	0	−1	5.290	5.289	0.001	<1
1	−1	−1	4.413	4.413	0.000	<1
1	1	−1	4.006	4.003	0.003	7
1	2	1	3.882	3.883	−0.000	3
2	1	0	3.726	3.723	0.003	7
1	1	2	3.686	3.683	0.003	9
0	0	2	3.620	3.621	−0.001	100
2	1	1	3.579	3.584	−0.005	3
1	2	0	3.541	3.541	0.000	6
0	2	0	3.437	3.439	−0.002	4
2	0	−1	3.340	3.340	0.000	12
1	0	−2	3.319	3.314	−0.003	15
2	0	1	3.209	3.206	0.003	6
2	2	1	3.152	3.152	0.000	7
2	1	−1	3.091	3.092	−0.001	5
1	−2	−1	3.021	3.026	−0.005	<1
2	2	0	2.984	2.986	−0.001	4
2	−1	0	2.901	2.900	0.000	4
2	1	2	2.868	2.867	0.001	7
2	2	2	2.803	2.803	−0.000	2
1	2	−1	2.759	2.759	−0.000	19
1	1	−2	2.722	2.723	−0.001	4
0	2	−1	2.690	2.692	−0.002	2
0	1	3	2.659	2.662	−0.003	2
1	3	1	2.643	2.643	−0.001	2
1	3	2	2.574	2.577	−0.002	2
1	1	3	2.552	2.550	0.002	5
2	0	2	2.514	2.513	0.000	10
2	1	−2	2.389	2.389	−0.000	3
1	−2	1	2.343	2.345	−0.001	2
3	1	−1	2.330	2.331	−0.001	2
3	3	1	2.104	2.105	−0.001	2
3	3	3	1.869	1.869	−0.000	24
0	0	4	1.810	1.810	−0.000	27
3	3	−1	1.773	1.775	−0.002	5

TABLE 3
Crystallographic Parameters

	$RbZn_2(HPO_4)_2(H_2PO_4)\cdot 2H_2O$	$RbZn(HPO_4)(H_2PO_4)\cdot H_2O$
Empirical formula	$RbZn_2P_3O_{14}H_8$	$RbZnP_2O_9H_5$
Formula weight	541.20	361.83
Crystal system	Orthorhombic	Triclinic
a (Å)	7.6458(9)	7.712(2)
b (Å)	9.965(2)	7.9824(7)
c (Å)	15.603(3)	8.0422(9)
α (degrees)	90	64.313(7)
β (degrees)	90	84.90(2)
γ (degrees)	90	72.364(9)
V (Å^3)	1189.8(3)	424.6(2)
Z	4	2
Space group	$P2_12_12_1$ (No. 19)	$P\bar{1}$ (No. 2)
T (°C)	25(2)	25(2)
λ (Mo$K\alpha$) (Å)	0.71073	0.71073
ρ_{calc} (g/cm^3)	3.03	2.83
μ (cm^{-1})	85.71	89.0
Total data	2646	4743
Observed data[a]	1695[b]	1794[c]
Parameters	183	119
$R(F)$[d]	3.90	3.97
$R_w(F)$[e]	3.91	4.24
S (goodness of fit)	1.90	1.90

[a] $I > 3\sigma(I)$ after data merging.
[b] $R_{Int} = 4.73\%$.
[c] $R_{Int} = 4.70\%$.
[d] $R = 100 \times \sum||F_o| - |F_c||/\sum|F_o|$.
[e] $R_w = 100 \times [\sum w(|F_o| - |F_c|)^2/\sum w|F_o|^2]^{1/2}$.

Starting coordinates for the heavy atoms in $RbZn_2(HPO_4)_2(H_2PO_4)\cdot 2H_2O$ were located by direct methods using the program SHELXS-86 (17) and the crystal-structure model was successfully developed in space group $P2_12_12_1$. The oxygen atom positions were readily located from difference Fourier maps and added to the structural model. No proton positions could be located from difference maps during the latter stages of refinement. The final cycles of full-matrix least-squares refinement (program CRYSTALS (18)), using complex, neutral-atom scattering factors from the "International Tables for Crystallography" (19) minimized the function $\sum w_i(F_o - F_c)^2$, with $w_i = 1/[\sigma(F)]^2$ and included anisotropic temperature factors for all atoms and a Larson-type secondary extinction correction (20). The absolute structure of the individual crystal studied was established by refining the Flack parameter (21) to $-0.02(1)$, and is as listed in the results section. Assuming the opposite absolute structure (Flack parameter fixed at 1.00) resulted in significantly higher residuals of $R = 6.10\%$ and $R_w = 5.89\%$. Because no asymmetric reagents were used in the synthesis, we may assume that the bulk sample of $RbZn_2(HPO_4)_2(H_2PO_4)\cdot 2H_2O$ consists of a random 50 : 50 mixture of crystals of both absolute structures.

After starting heavy-atom coordinates were located by direct methods, the structure of $RbZn(HPO_4)(H_2PO_4)\cdot H_2O$ was developed in the centrosymmetric space group $P\bar{1}$ (No. 2) which was assumed for the remainder of the refinement procedure. Oxygen atoms were located from difference maps and added to the refinement. No proton positions could be located. Supplementary tables of anisotropic thermal factors and observed and calculated structure factors for $RbZn_2(HPO_4)_2(H_2PO_4)\cdot 2H_2O$ and $RbZn(HPO_4)(H_2PO_4)\cdot H_2O$ are available from the authors.

RESULTS

Crystal Structure of $RbZn_2(HPO_4)_2(H_2PO_4)\cdot 2H_2O$

Final atomic positional and thermal parameters for $RbZn_2(HPO_4)_2(H_2PO_4)\cdot 2H_2O$ are listed in Table 4, with selected bond distance and angle data in Table 5. $RbZn_2(HPO_4)_2(H_2PO_4)\cdot 2H_2O$ is a layered phase with respect to Zn–O–P and Zn–O–Zn bonds, built up from irregularly coordinated rubidium cations, octahedral ZnO_6, and tetrahedral ZnO_4 and PO_4 centers. The building unit of $RbZn_2(HPO_4)_2(H_2PO_4)\cdot 2H_2O$ and atom labeling scheme is illustrated in Fig. 1 with CAMERON (22), and the complete crystal structure is shown in Fig. 2.

The rubidium cation in $RbZn_2(HPO_4)_2(H_2PO_4)\cdot 2H_2O$ is coordinated by 11 oxygen atoms within 3.5 Å and an average Rb(1)–O bond distance of 3.170(3) Å results for the irregular RbO_{11} polyhedron. The bond valence sum (BVS) for rubidium, calculated according to the formalism of Brown (23), is 1.03 (expected value = 1.00), indicating that in terms of size, the rubidium cation is well suited to its interlayer site. The two zinc atoms in $RbZn_2(HPO_4)_2(H_2PO_4)\cdot 2H_2O$ show distinct structural behavior: Zn(1) is octahedrally coordinated by O atoms, with a resulting d_{av}[Zn(1)–O] of 2.133(4) Å (based on a wide spread of Zn–O distances as listed in Table 5; mean error was calculated according to (24)) and BVS[Zn(1)] of 1.98 (expected: 2.00). Zn(1) makes three Zn–O–P bonds, one Zn–O–(P, Zn) link, and also coordinates directly to two water-molecule oxygen atoms which are in *cis* configuration. The second distinct zinc atom is tetrahedral, with d_{av}[Zn(2)–O] = 1.950(4) Å and BVS[Zn(2)] = 2.06. This species makes four Zn–O–P linkages *via* bridging oxygen atoms. The three PO_4 centers in $RbZn_2(HPO_4)_2(H_2PO_4)\cdot 2H_2O$ are all fairly regular tetrahedra. P(1) makes linkages to both Zn(1) and Zn(2) *via* the triply coordinated oxygen atom O(2), as well as a single link to Zn(1) *via* O(4). Its two remaining vertices, O(10) and O(11), are bonded only to P(1). The $P(2)O_4$ group makes one link to Zn(1) *via* O(1), two links to different Zn(2) species *via* O(7) and O(8), and one "terminal" P(2)–O(12) bond. P(3) forms bicoordinate bridges to Zn(1) (*via* O(3)) and Zn(2) (*via* O(9)), and has two terminal-oxygen-atom partners, O(13) and O(14). Average P–O bond distances (with BVS values in parentheses, compared to an expected value of 5.00) of 1.530(4) Å (5.10), 1.535(4) Å (5.03), and 1.540(4) Å (4.95) result for P(1), P(2), and P(3), respectively. The oxygen atoms divide into bicoordinate Zn–O–P bridges [O(1), O(3), O(4), O(7), O(8) and O(9)] with θ_{av}[Zn–O–P] = 134°; a tricoordinate species, O(2), which links to Zn(1), Zn(2), and P(2), and the terminal O atoms O(10) to O(14). The "overbonded" situation of O(2) is perhaps responsible for the very long octahedral Zn(1)–O(2) bond length of 2.384(8) Å. Charge balancing of the $[Zn_2P_3O_{14}]^{9-}$ layer stoichiometry requires eight

TABLE 4
Final Atomic Coordinates/Thermal Factors for $RbZn_2(HPO_4)_2(H_2PO_4)\cdot 2H_2O$

Atom	*x*	*y*	*z*	U_{eq}[a]
Rb(1)	0.3464(2)	0.0665(1)	1.02596(8)	0.0284
Zn(1)	0.5540(2)	0.3664(1)	0.69823(8)	0.0154
Zn(2)	0.8790(2)	0.1156(1)	0.69874(8)	0.0149
P(1)	0.6634(4)	0.1361(3)	0.8631(2)	0.0132
P(2)	0.8351(4)	−0.1979(3)	0.7123(2)	0.0134
P(3)	0.6423(4)	0.1599(3)	0.5411(2)	0.0138
O(1)	0.356(1)	0.3287(8)	0.7811(4)	0.0165
O(2)	0.689(1)	0.1819(8)	0.7694(4)	0.0126
O(3)	0.513(1)	0.2262(8)	0.6023(4)	0.0113
O(4)	0.437(1)	0.5102(8)	0.6276(5)	0.0174
O(5)	0.648(1)	0.5015(7)	0.7968(5)	0.0183
O(6)	0.816(1)	0.394(1)	0.6546(4)	0.0235
O(7)	0.947(1)	−0.0715(8)	0.7248(4)	0.0154
O(8)	1.105(1)	0.1932(8)	0.7262(4)	0.0174
O(9)	0.800(1)	0.0978(8)	0.5811(4)	0.0161
O(10)	0.838(1)	0.1317(9)	0.9080(4)	0.0183
O(11)	0.558(1)	0.2518(8)	0.9101(4)	0.0161
O(12)	0.864(1)	−0.2510(9)	0.6168(4)	0.0205
O(13)	0.705(1)	0.2720(8)	0.4754(5)	0.0216
O(14)	0.534(1)	0.0543(8)	0.4902(4)	0.0196

[a] U_{eq} (Å^2) = 1/3[$U_1 + U_2 + U_3$].

TABLE 5
Selected Bond Distances (Å) and Angles (°) for $RbZn_2(HPO_4)_2(H_2PO_4)\cdot 2H_2O$

Rb(1)–O(4)	2.966(8)	Rb(1)–O(5)	3.227(8)
Rb(1)–O(7)	3.482(8)	Rb(1)–O(9)	3.278(8)
Rb(1)–O(10)	3.180(9)	Rb(1)–O(11)	3.050(8)
Rb(1)–O(11)	3.022(8)	Rb(1)–O(12)	3.294(8)
Rb(1)–O(12)	3.209(9)	Rb(1)–O(13)	2.960(8)
Rb(1)–O(14)	3.198(8)		
Zn(1)–O(1)	2.026(7)	Zn(1)–O(2)	2.384(8)
Zn(1)–O(3)	2.071(7)	Zn(1)–O(4)	2.017(8)
Zn(1)–O(5)	2.166(8)	Zn(1)–O(6)	2.134(8)
Zn(2)–O(2)	1.936(8)	Zn(2)–O(7)	1.978(8)
Zn(2)–O(8)	1.942(8)	Zn(2)–O(9)	1.942(7)
P(1)–O(2)	1.545(7)	P(1)–O(4)	1.478(8)
P(1)–O(10)	1.510(8)	P(1)–O(11)	1.585(8)
P(2)–O(1)	1.488(8)	P(2)–O(7)	1.534(8)
P(2)–O(8)	1.520(8)	P(2)–O(12)	1.597(7)
P(3)–O(3)	1.526(7)	P(3)–O(9)	1.488(8)
P(3)–O(13)	1.589(8)	P(3)–O(14)	1.557(8)
Zn(1)–O(1)–P(2)	144.2(5)	Zn(1)–O(2)–Zn(2)	108.9(3)
Zn(1)–O(2)–P(1)	127.7(5)	Zn(2)–O(2)–P(1)	122.3(5)
Zn(1)–O(3)–P(3)	130.2(5)	Zn(1)–O(4)–P(1)	141.3(5)
Zn(2)–O(7)–P(2)	127.0(4)	Zn(2)–O(8)–P(2)	133.8(5)
Zn(2)–O(9)–P(3)	127.6(5)		

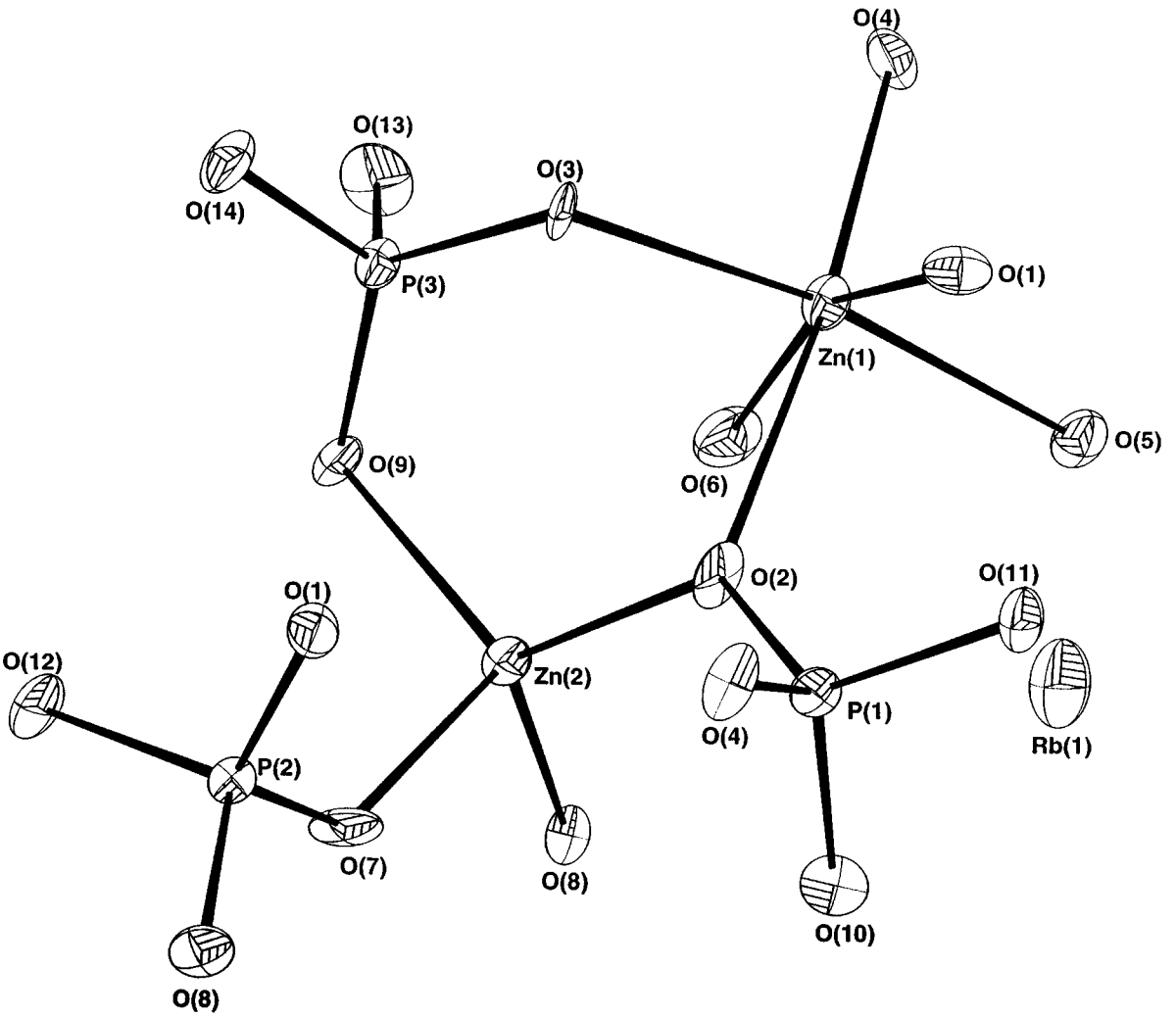

FIG. 1. View of a fragment of the $RbZn_2(HPO_4)_2(H_2PO_4)\cdot 2H_2O$ structure showing the atom labeling scheme (50% thermal ellipsoids).

protons in addition to the extra-layer rubidium cation. We suggest that four of these are accounted for by two water molecules coordinated to Zn (oxygen atoms O(5) and O(6)) and four more are distributed over various terminal P–O links present in $RbZn_2(HPO_4)_2(H_2PO_4)\cdot 2H_2O$ (oxygen atoms O(10) to O(14)). These terminal P–OH bonds show their characteristic lengthening, relative to unprotonated P–O bonds (25), and have individual bond valences in the range 1.0 to 1.2.

The polyhedral connectivity of the ZnO_6, ZnO_4, and PO_4 centers in $RbZn_2(HPO_4)_2(H_2PO_4)\cdot 2H_2O$ leads to a layered structural *motif*, in which anionic sheets of stoichiometry $[Zn_2(HPO_4)_2(H_2PO_4)\cdot 2H_2O]^-$ are arranged normal to the [001] direction. These sheets are built up from vertex-sharing zigzag chains of alternating $Zn(2)O_4$ and $HP(2)O_4$ groups which propagate in the [001] direction. These chains are crosslinked in the *b* direction by the $Zn(1)O_4(H_2O)_2$ octahedra. Each $Zn(1)O_4(H_2O)_2$ unit links from zinc to phosphorus, resulting in unusual polyhedral "eight-rings" which contain five zinc atoms and three phosphorus atoms (Fig. 3) and thus include both Zn–O–Zn and Zn–O–P links but no P–O–P linkages. The $P(1)O_4$ and $P(3)O_4$ groups complete the layered *motif* in $RbZn_2(HPO_4)_2(H_2PO_4)\cdot 2H_2O$. P(1) bonds to the Zn(1)–O(2)–Zn(2) oxygen bridge and also to a nearby octahedral zinc center. P(3) makes P–O–Zn bonds to an octahedral and a tetrahedral zinc center. Crystal symmetry dictates that both these P atoms bond to both faces of a particular *ab*-plane sheet, with the P(3)-centered groups projecting into the interlayer region. Interlayer rubidium cations complete the structure by occupying pseudo-channels propagating in the [100] direction between the *ab*-plane sheets. There are also probable interlayer hydrogen bonding interactions, as P(3)–OH ⋯ O links.

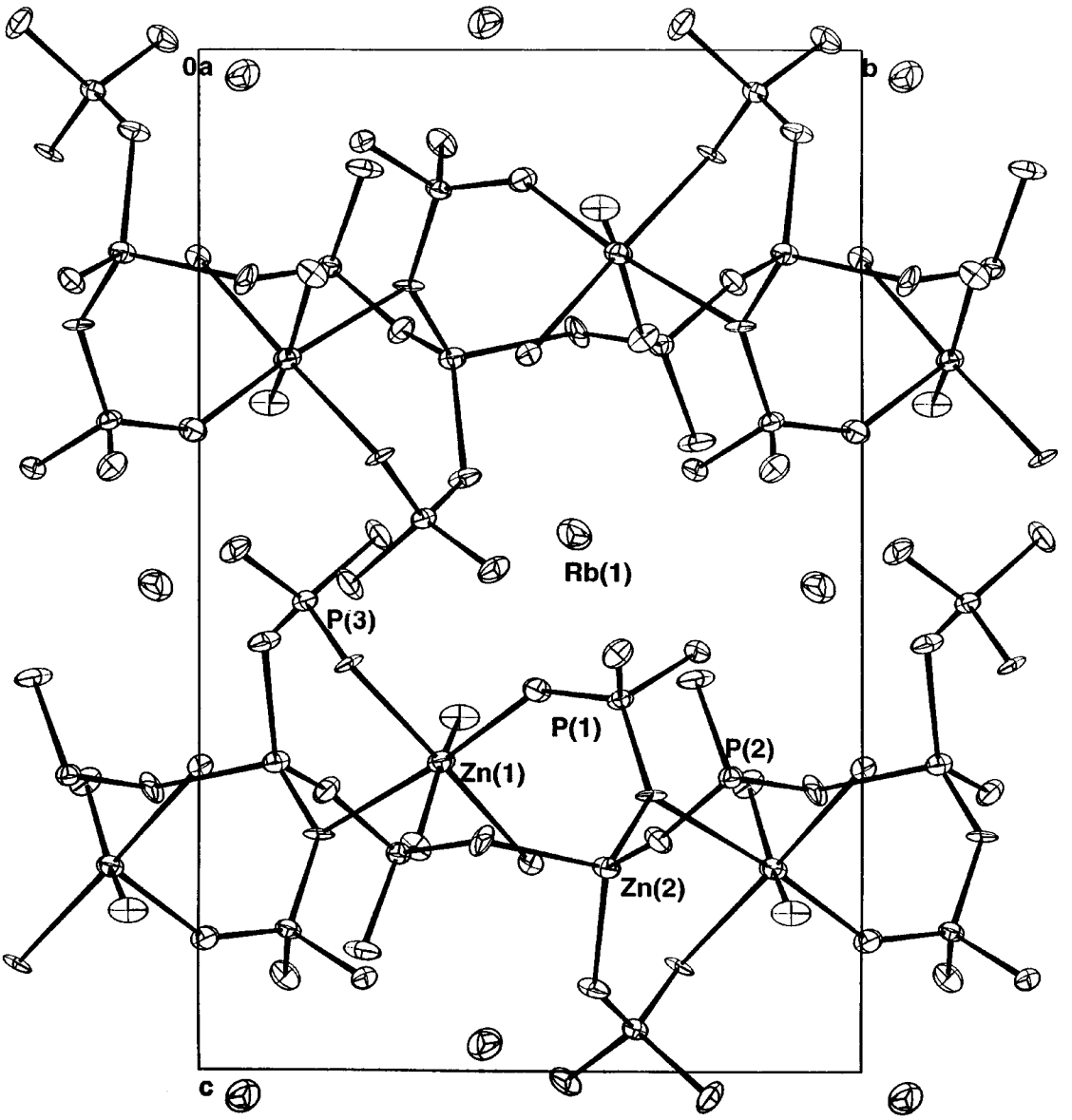

FIG. 2. View down [100] of the unit cell of $RbZn_2(HPO_4)_2(H_2PO_4)\cdot 2H_2O$ showing the anionic layers separated by rubidium cations.

Crystal Structure of $RbZn_2(HPO_4)_2(H_2PO_4)\cdot 2H_2O$

Final atomic positional and thermal parameters for $RbZn(HPO_4)(H_2PO_4)\cdot H_2O$ are listed in Table 6, with selected bond distance and angle data in Table 7. $RbZn(HPO_4)(H_2PO_4)\cdot H_2O$ is a one-dimensional (or "polymeric") phase with respect to Zn–O–P bonds and is built up from irregularly coordinated rubidium cations and tetrahedral ZnO_4 and PO_4 centers. The building unit of $RbZn(HPO_4)(H_2PO_4)\cdot H_2O$ and atom labeling scheme is shown in Fig. 4, and the complete crystal structure is illustrated in Fig. 5.

The rubidium cation in $RbZn(HPO_4)(H_2PO_4)\cdot H_2O$ is irregularly coordinated by eight oxygen atoms within 3.4 Å with an average Rb(1)–O bond distance of 3.072(2) Å, and a BVS(Rb) of 0.94. The single zinc cation is tetrahedral with d_{av}[Zn(1)–O] = 1.940(3) Å; Zn(1) makes four Zn–O–P bonds to different nearby P atoms. The two PO_4 centers in $RbZn(HPO_4)(H_2PO_4)\cdot H_2O$ are both fairly regular tetrahedra: P(1) and P(2) both make two P–O–Zn linkages and have two terminal P–O vertices (Table 7). Average P–O bond distances of 1.536(3) and 1.542(3) Å result for P(1) and P(2), respectively. Bond valence sums of 2.12 for Zn(1), 5.00 for P(1), and 4.91 for P(2) are typical. The oxygen atoms

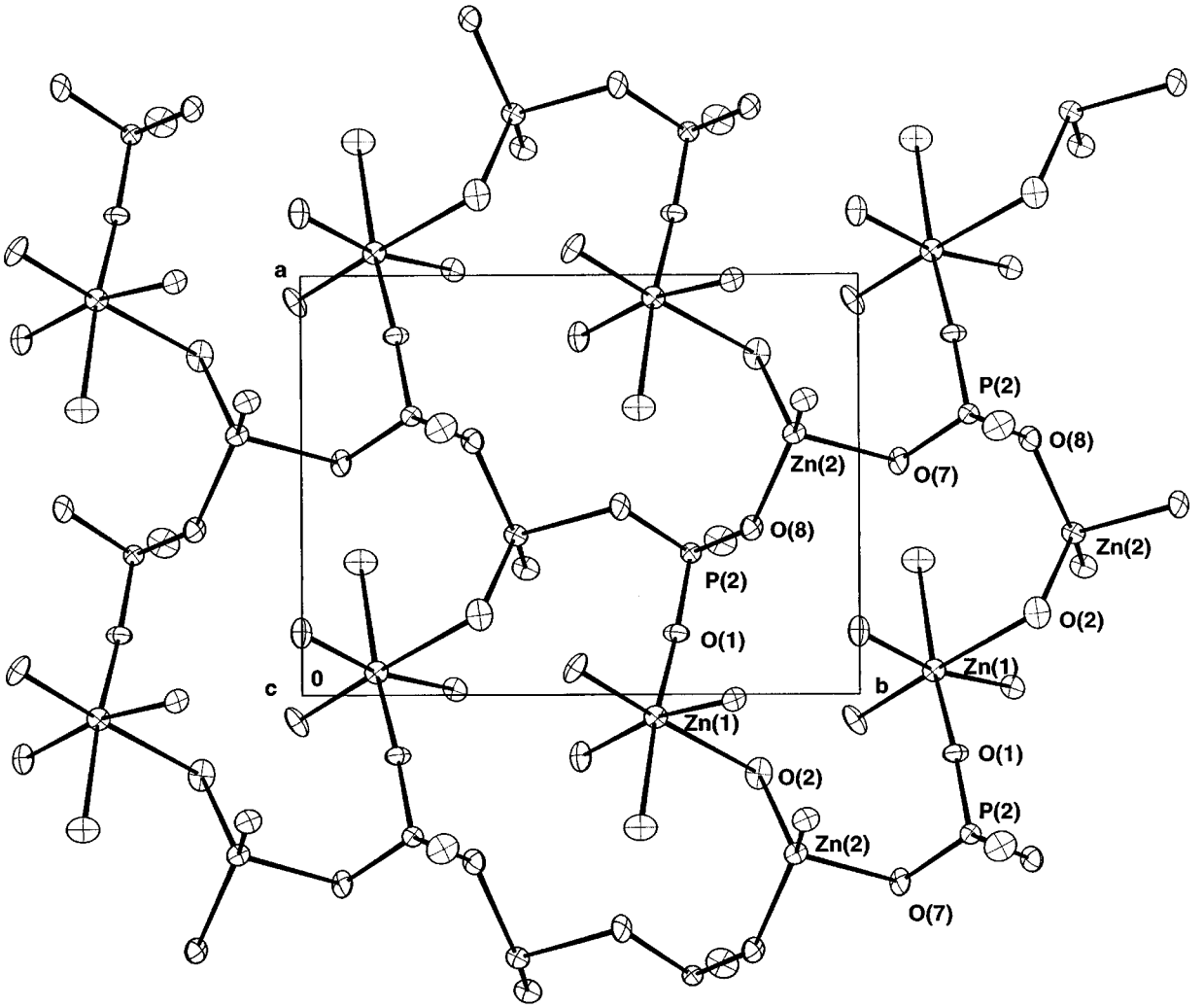

FIG. 3. View down [001] of a zincophosphate layer in $RbZn_2(HPO_4)_2(H_2PO_4)\cdot 2H_2O$, showing the actahedral/tetrahedral "8-ring" formed by the connection of octahedral and tetrahedral subunits (see text). P(1)- and P(3)-centered tetrahedra are omitted for clarity.

divide into bicoordinate Zn–O–P bridges [O(1), O(2), O(3), O(4)] with θ_{av}[Zn–O–P] = 130.3°, the terminal O atoms O(5) to O(8), and an extra-chain water molecule [O(9)]. Charge balancing of the $[ZnP_2O_8]^{4-}$ chain stoichiometry requires three protons, in addition to the extra-layer rubidium cation. Neglecting the possibility of the extra framework O(9) species being part of a hydronium cation, then three of the four terminal P–O vertices must be protonated. Bond valence/bond distance considerations suggest that the P(1)–O(5), P(2)–O(7), and P(2)–O(8) bonds bear protons; i.e., $RbZn(HPO_4)(H_2PO_4)\cdot H_2O$ contains ordered $HP(1)O_4$ and $H_2P(2)O_4$ groups.

The structure of $RbZn(HPO_4)(H_2PO_4)\cdot H_2O$ consists of infinite chains of vertex-sharing tetrahedra propagating in the [100] direction. These chains (Fig. 6) are built up from 4-rings of alternating Zn- and P-centered tetrahedra. The zinc center serves to link the 4-rings into an infinite chain; the hydrogen phosphate and dihydrogen phosphate groups segregate into their own 4-rings. These anionic chains are crosslinked by the rubidium cation and by probable H bonding interactions between P–OH entities and the extra-chain water molecule.

Physical Properties

TGA for $RbZn_2(HPO_4)_2(H_2PO_4)\cdot 2H_2O$ showed a gradual weight loss of 13% over the range ~85–500°C. The calculated weight loss for the nominal elimination of four water molecules from this phase to leave a residue of "$RbZn_2P_3O_{10}$" is 13.3%. An endothermic DTA trace suggested that this decomposition occurs in at least three distinct steps. TGA for $RbZn(HPO_4)(H_2PO_4)\cdot H_2O$ showed

TABLE 6
Final Atomic Coordinates / Thermal Factors for $RbZn(HPO_4)(H_2PO_4)\cdot H_2O$

Atom	x	y	z	U_{eq}[a]
Rb(1)	0.8632(1)	0.7279(1)	0.7761(1)	0.0267
Zn(1)	0.7397(1)	0.2649(1)	0.9729(1)	0.0138
P(1)	0.3821(2)	0.5492(2)	0.7477(2)	0.0126
O(2)	1.0762(2)	0.1815(2)	0.7438(2)	0.0128
O(1)	0.5262(6)	0.3507(6)	0.8178(7)	0.0205
O(2)	0.7724(6)	−0.0054(6)	1.1382(7)	0.0180
O(3)	0.7332(6)	0.4302(6)	1.0953(6)	0.0178
O(4)	0.9663(6)	0.2958(6)	0.8477(7)	0.0200
O(5)	0.4824(7)	0.7124(7)	0.6753(6)	0.0197
O(6)	0.2627(6)	0.5806(6)	0.5909(6)	0.0185
O(7)	1.1596(6)	0.3141(6)	0.5731(6)	0.0157
O(8)	0.9485(6)	0.1121(6)	0.6605(6)	0.0200
O(9)	0.5564(6)	0.0751(6)	0.6869(7)	0.0217

[a] U_{eq} (Å^2) $= 1/3[U_1 + U_2 + U_3]$.

TABLE 7
Selected Bond Distances (Å) and Angles (°) for $RbZn(HPO_4)(H_2PO_4)\cdot H_2O$

Rb(1)–O(3)	2.990(4)	Rb(1)–O(3)	3.067(5)
Rb(1)–O(4)	3.091(4)	Rb(1)–O(4)	3.313(5)
Rb(1)–O(5)	3.167(5)	Rb(1)–O(7)	2.995(5)
Rb(1)–O(8)	3.057(5)	Rb(1)–O(9)	2.898(4)
Zn(1)–O(1)	1.918(5)	Zn(1)–O(2)	1.931(4)
Zn(1)–O(3)	1.947(5)	Zn(1)–O(4)	1.965(5)
P(1)–O(1)	1.527(4)	P(1)–O(3)	1.518(4)
P(1)–O(5)	1.583(5)	P(1)–O(6)	1.514(5)
P(2)–O(2)	1.512(4)	P(2)–O(4)	1.522(4)
P(2)–O(7)	1.554(5)	P(2)–O(8)	1.580(5)
Zn(1)–O(1)–P(1)	127.4(3)	Zn(1)–O(2)–P(2)	138.3(3)
Zn(1)–O(3)–P(1)	128.9(3)	Zn(1)–O(4)–P(2)	126.5(3)

a gradual weight loss of 11.4% over the range ~85–570°C. The calculated weight loss for the nominal elimination of 2.5 water molecules from this phase to leave a residue of "$RbZnP_2O_{6.5}$" is 12.4%.

CONCLUSIONS

Two new rubidium zinc phosphate hydrates, $RbZn_2(HPO_4)_2(H_2PO_4)\cdot 2H_2O$ and $RbZn(HPO_4)(H_2PO_4)\cdot H_2O$, have been prepared by solution-phase methods and structurally characterized by single-crystal X-ray methods.

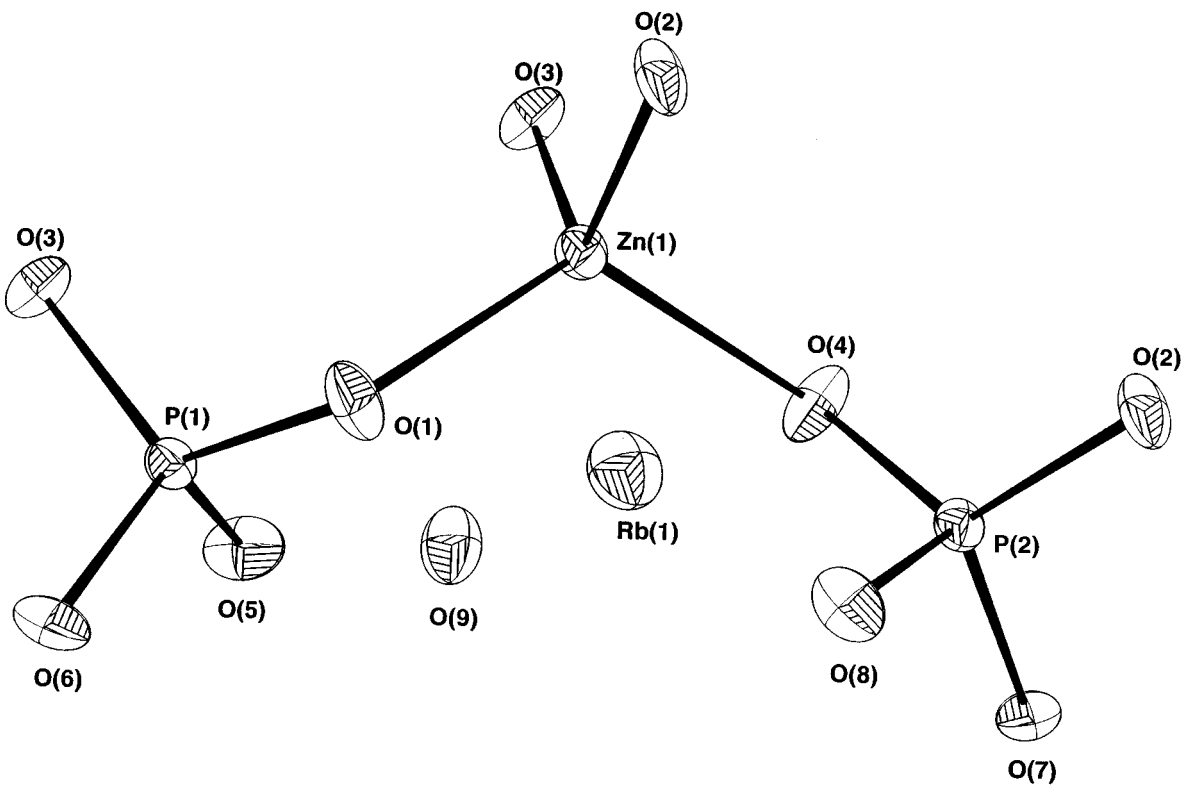

FIG. 4. View of a fragment of the $RbZn(HPO_4)(H_2PO_4)\cdot H_2O$ structure showing the atom labeling scheme (50% thermal ellipsoids).

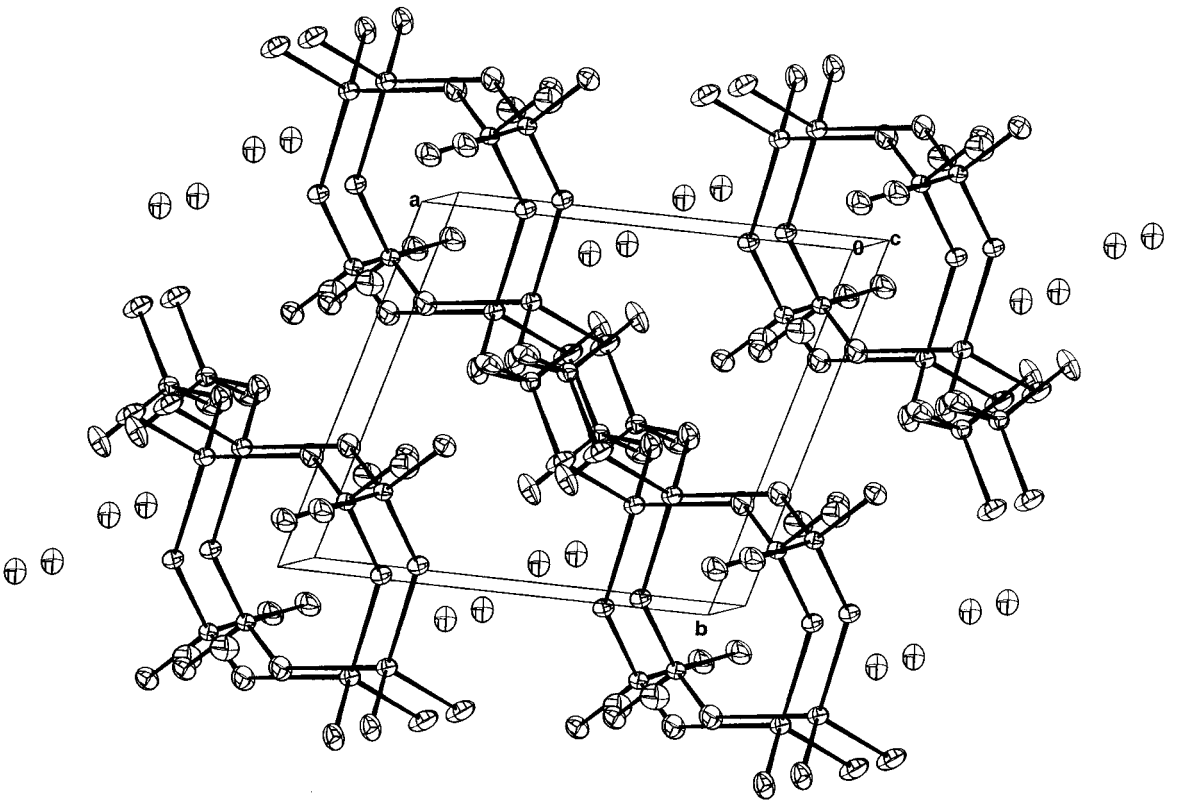

FIG. 5. View down [001] of the $RbZn(HPO_4)(H_2PO_4)\cdot H_2O$ crystal structure.

The coexistence of octahedral and tetrahedral zinc centers and the vertex-linked connectivity of the $ZnO_4(H_2O)_2$, ZnO_4, and PO_4 groups in $RbZn_2(HPO_4)_2(H_2PO_4)\cdot 2H_2O$ is somewhat reminiscent of the situation in the mineral species hopeite, $Zn_3(PO_4)_2\cdot 4H_2O$ (26), which is built up from similar octahedral and tetrahedral units. In hopeite, the octahedral zinc atoms (with *cis*-coordinated water molecules, as in $RbZn_2(HPO_4)_2(H_2PO_4)\cdot 2H_2O$) serve to bridge complex anionic tetrahedral layers into a three-dimensional structure. The tricoordinate O atom in

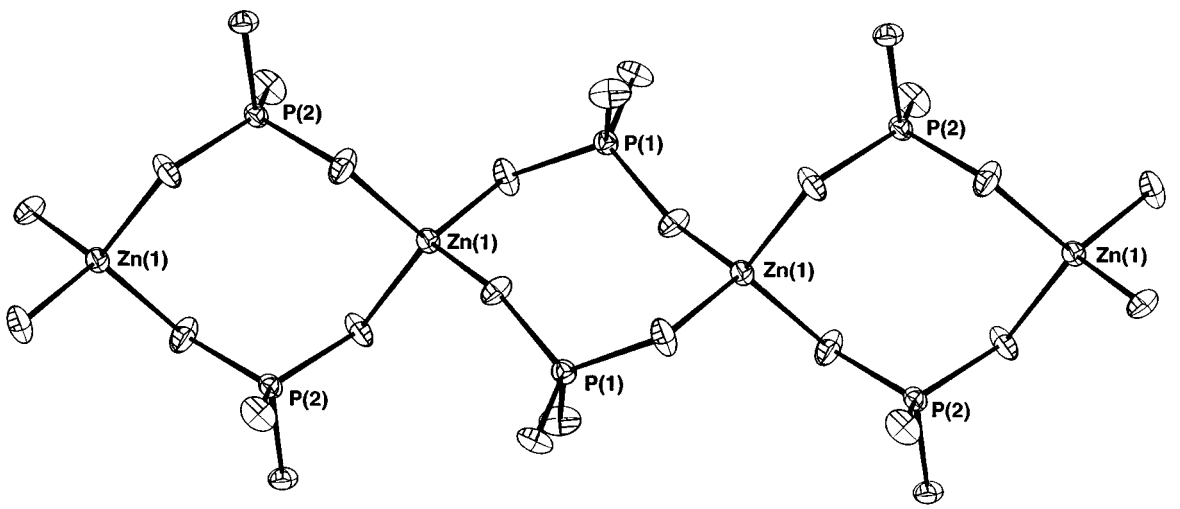

FIG. 6. Detail of the $RbZn(HPO_4)(H_2PO_4)\cdot H_2O$ structure, showing the infinite chain of 4-rings. Note that the P(1)- (hydrogen phosphate) and P(2)-centered (dihydrogen phosphate) groups segregate into their own 4-rings.

$RbZn_2(HPO_4)_2(H_2PO_4)\cdot 2H_2O$ has been seen in several other framework zincophosphates (8, 10). In each case, this results in the presence of Zn–O–Zn bonds as well as Zn–O–P bonds. In some phases, such as $NH(CH_3)_3\cdot Zn_4(H_2O)(PO_4)_3$ (10), this bonding situation leads to infinite chains of –Zn–O–Zn–O– bonds. In $RbZn_2(HPO_4)_2(H_2PO_4)\cdot 2H_2O$, however, the zinc to zinc linkage is not continuous throughout the structure and results in nominal Zn_2O_9 "dimers".

$RbZn(HPO_4)(H_2PO_4)\cdot H_2O$ is isostructural with synthetic $NH_4Zn(HPO_4)(H_2PO_4)\cdot H_2O$ (27). The zincophosphate chain geometries are very similar in the two phases. An average $N\cdots O$ bond distance of 2.98 Å arises for the nominal eight-coordinated ammonium cation in $NH_4Zn(HPO_4)(H_2PO_4)\cdot H_2O$, compared to 3.07 Å for the equivalent average Rb–O distance in $RbZn(HPO_4)(H_2PO_4)\cdot H_2O$. The polymeric chain *motif* of fused tetrahedral 4-rings is uncommon, but it has also been observed in zinc diethylphosphate (28) and related phases.

ACKNOWLEDGMENT

We thank the Australian Research Council for financial support.

REFERENCES

1. T. E. Gier, W. T. A. Harrison, T. M. Nenoff, and G. D. Stucky, "Synthesis of Microporous Materials, Volume 1: Molecular Sieves" (M. L. Occelli and H. E. Robson, Eds.), pp. 407–426. Van Nostrand Reinhold, New York, 1992.
2. W. T. A. Harrison, T. E. Gier, K. L. Moran, J. M. Nicol, H. Eckert, and G. D. Stucky, *Chem. Mater.* **3,** 27 (1991).
3. T. M. Nenoff, W. T. A. Harrison, T. E. Gier, and G. D. Stucky, *J. Am. Chem. Soc.* **113,** 378 (1991).
4. W. T. A. Harrison, R. W. Broach, R. A. Bedard, T. E. Gier, X. Bu, and G. D. Stucky, *Chem. Mater.* **8,** 691 (1996). [and references therein]
5. W. T. A. Harrison, T. E. Gier, G. D. Stucky, R. W. Broach, and R. A. Bedard, *Chem. Mater.* **8,** 145 (1996).
6. W. T. A. Harrison, T. M. Nenoff, T. E. Gier, and G. D. Stucky, *J. Solid State Chem.* **113,** 168 (1994).
7. W. T. A. Harrison, T. M. Nenoff, T. E. Gier, and G. D. Stucky, *Inorg. Chem.* **32,** 2437 (1993).
8. T. Song, M. B. Hursthouse, J. Chen, J. Xu, K. M. A. Malik, R. H. Jones, R. Xu, and J. M. Thomas, *Adv. Mater.* **6,** 679 (1994).
9. P. Feng, X. Bu, and G. D. Stucky, *Angew. Chem.* **34,** 1745 (1995).
10. X. Bu, P. Feng, and G. D. Stucky, *J. Solid State Chem.* **125,** 243 (1996).
11. W. T. A. Harrison and M. L. F. Phillips, *Chem. Commun.* 2781 (1996).
12. W. T. A. Harrison and L. Hannooman, *Angew. Chem. Int. Ed. Engl.* **36,** 640 (1997).
13. M. T. Averbuch-Pouchot, *Zeit. Kristallogr.* **171,** 113 (1985).
14. L. Elammari and B. Elouadi, *J. Chim. Phys. Phys.–Chim. Biol.* **88,** 1969 (1991).
15. K. Yvon, W. Jeitschko, and E. Parthe, *J. Appl. Crystallogr.* **10,** 73 (1977).
16. T. J. B. Holland and S. A. T. Redfern, Program UNITCELL, Univ. of Cambridge, UK.
17. G. M. Sheldrick, "SHELXS86 User Guide." Univ. of Göttingen, Germany.
18. D. J. Watkin, J. R. Carruthers, and P. W. Betteridge, "CRYSTALS User Guide." Chemical Crystallography Laboratory, Univ. of Oxford, UK.
19. "International Tables for Crystallography," Volume IV. Kynoch Press, Birmingham, UK.
20. A. C. Larson, *Acta Crystallogr.* **23,** 664 (1967).
21. H. D. Flack, *Acta Crystallogr. A* **39,** 876 (1983).
22. L. J. Pearce, D. J. Watkin, and C. K. Prout, "CAMERON User Guide." Chemical Crystallography Laboratory, Univ. of Oxford, UK.
23. I. D. Brown, Program VALENCE, Institute for Materials Research, McMaster University, Canada.
24. J. R. Taylor, "An Introduction to Error Analysis." University Science Books/Oxford Univ. Press, London, 1982.
25. P. Lightfoot and D. Masson, *Acta Crystallogr. C* **52,** 1077 (1996).
26. A. Whitaker, *Acta Crystallogr. B* **31,** 2026 (1975).
27. A. Boudjada, D. Tranqui, and J. C. Guitel, *Acta Crystallogr. B* **36,** 1176 (1980).
28. W. T. A. Harrison, T. M. Nenoff, T. E. Gier, and G. D. Stucky, *Inorg. Chem.* **31,** 5395 (1992).